

The Dopamine D2R Antagonist Trifluoperazine Suppresses High-Fat Diet-Induced Hyperglycemia and Hypothalamic Gliosis in Obese Mice

Hui-Ting Huang

Institute of Life Sciences, College of Bioscience and Biotechnology, National Cheng Kung University

Pei-Chun Chen

Institute of Physiology, College of Medicine, National Cheng Kung University

Po-See Chen

Department of Psychiatry, College of Medicine, National Cheng Kung University

Wen-Tai Chiu

Department of Biomedical Engineering, College of Engineering, National Cheng Kung University

Yu-Min Kuo

Institute of Basic Medical Sciences, Department of Cell Biology and Anatomy, College of Medicine, National Cheng Kung University

Shun-Fen Tzeng (✉ stzeng@mail.ncku.edu.tw)

Institute of Life Sciences, College of Bioscience and Biotechnology, National Cheng Kung University

Research Article

Keywords: Inflammation, cytokine, microglia, gliosis, dopamine receptor

Posted Date: April 12th, 2021

DOI: <https://doi.org/10.21203/rs.3.rs-382784/v1>

License: © ⓘ This work is licensed under a Creative Commons Attribution 4.0 International License.

[Read Full License](#)

Abstract

Microglia, the resident macrophages of the central nervous system (CNS), as well as astrocytes, are CNS glia cells to support neurodevelopment and neuronal function. Yet, their activation-associated with CNS inflammation is involved in the initiation and progression of neurological disorders. Mild inflammation in the periphery and glial activation called gliosis in the hypothalamic region, arcuate nucleus (ARC), are generally observed in the obese individuals and animal models. Thus, reduction in peripheral and central inflammation is considered as a strategy to lessen the abnormality of obesity-associated metabolic indices. In this study, we reported that acute peripheral challenge by inflammagen lipopolysaccharide (LPS) triggered an upregulation of hypothalamic dopamine type 2 receptor (D2R) expression, and chronic feeding by high fat diet (HFD) caused an increased levels of D2R in the ARC. The in vitro and in vivo studies indicated that a D2R antagonist named trifluoperazine (TFP) was able to suppress LPS-stimulated activation of microglia and effectively inhibited LPS-induced peripheral inflammation, as well as hypothalamic inflammation. Further findings showed daily peripheral administration intraperitoneally (i.p.) by TFP for 4 weeks was able to reduce the levels of plasma and hypothalamic tumor necrosis factor- α (TNF- α) and interleukin-1 β (IL-1 β) in obese mice receiving HFD for 16 weeks. Moreover, plasma glucose and insulin were effectively decreased by daily treatment with TFP for 4 weeks. In parallel, microglia and astrocytes in the ARC was also inhibited by peripheral administration by TFP. According to our results, TFP has the ability to suppress HFD-induced hyperglycemia, inflammation and gliosis in hypothalamus.

Introduction

Obesity caused by excessive dietary intake is not only a causal factor in the development of cardiovascular disease but also a harmful stimulus that induces neurodegeneration in the central nervous system (CNS) and cognitive dysfunction ¹. The hypothalamus is critical for regulating food intake and energy expenditure ². The hypothalamus consists of two centers, including a satiety center and a feeding center, which reciprocally coordinate to maintain a set point for body weight control. Among hypothalamic nuclei, paraventricular nuclei and arcuate nuclei (ARC) are important for neuroendocrine regulation and secrete hormone-releasing hormone to act on the anterior pituitary gland for hormone release ³.

Chronic systemic low-grade inflammation is a hallmark of obesity ^{4,5}. The inflammatory cytokines (i.e., TNF- α , IL-1 β , IL-6, CRP, and TLRs) have been detected in the plasma of obese individuals and fat-fed animals. Notably, obesity-associated brain inflammation occurs significantly in the hypothalamus ^{1,6,7}. In a rodent study, hypothalamic inflammation occurred at the onset of high-fat diet (HFD) feeding ^{8,9}. Gliosis, a reactive change in astrocytes (CNS supporting cell population) and microglia (CNS resident macrophages), also occurs in the hypothalamus of obese rodents and humans ^{8,9}. An increase in microglia and astrocyte hypertrophy can be observed in the ARC upon exposure to HFD, suggesting that gliosis is involved in HFD-induced leptin and insulin resistance and disturbance of energy homeostasis

¹⁰. Examination of cytokine expression in HFD-fed rats has shown that proinflammatory cytokines (IL-6 and TNF- α) were increased in the hypothalamus within 1–3 days after HFD feeding ^{8,11}. Similar observations have reported that IL-1 β expression was upregulated in the hypothalamus at 3 day after initiation of HFD feeding in mice ⁹. However, the expression of these proinflammatory cytokines in rats and mice declines in the weeks after HFD feeding ⁹. Nevertheless, prolonged microglial activation and demyelination were observed in the ARC of mice treated with chronic HFD feeding for months ¹². Thus, the inhibition of hypothalamic inflammation is considered an effective strategy for the control of glucose homeostasis ^{1,13}.

Trifluoperazine (TFP), a prescribed antipsychotic drug that has been used to suppress psychotic activity by inhibiting the postsynaptic dopamine receptor ¹⁴, not only has an immunosuppressive ability to inhibit cytokine production and release in immune cells ^{15,16} but also shows anticancer effects through different signaling pathways ¹⁷. Thus, the aim of the study was to determine whether TFP has a potential effect on the attenuation of HFD-induced inflammation. Although TFP did not attenuate the body weight of obese mice induced by chronic HFD feeding, the *in vivo* findings in conjunction with the *in vitro* observation that exposure to TFP significantly reduced LPS-induced proinflammatory cytokine expression in primary microglia demonstrate that treatment with TFP effectively attenuated HFD-induced elevation in blood glucose, systemic inflammation, and ARC gliosis.

Results

Trifluoperazine attenuates the production of proinflammatory mediators induced by inflammation challenge

An *in vitro* study using primary microglia prepared from rat pups at PD 1-2 was first conducted. As shown in Fig. 1A exposure to TFP at 1 mM for 3 h reduced iNOS immunoreactivity in IB4⁺-microglia under 10 ng/ml of LPS stimulation. We found that iNOS⁺-microglia in the culture only treated with LPS displayed an amoeboid shape (Fig. 1A, arrowheads), whereas microglia co-treated with LPS and TFP had a strong IB4 staining exhibited extending cell processes (Fig. 1A, arrows). Moreover, 1 mM of TFP induced the downregulation of proinflammatory cytokines, TNF- α and IL-1b in LPS-stimulated microglia (Fig. 1B). The results from hypothalamic mixed glia stimulated by LPS also indicated that TFP significantly inhibited LPS-induced release of the proinflammatory cytokines (i.e. TNF- α and IL-1b) in the cultures (Fig. 1C). Accordingly, the anti-inflammatory ability of TFP in microglia and mixed glia was validated.

Peripheral acute challenge with 1 mg/kg LPS is able to trigger systemic inflammation and hypothalamic microglial activation ¹⁸⁻²⁰. Accordingly, further experiments involving the co-administration of LPS with TFP (2 mg/kg) in mice via the i.p. route were designed to examine proinflammatory cytokines in the plasma and hypothalamus, as well as hypothalamic D2R mRNA expression. The plasma levels of TNF- α and IL-1b proteins were significantly elevated at 3 h and 6 h post LPS injection (Fig. 2A). This upregulation of TNF- α and IL-1b at the plasma level was effectively diminished by TFP. In parallel, the

results also showed that TFP downregulated LPS-stimulated expression of the two proinflammatory cytokine genes in the hypothalamus at 6 h post injection (Fig. 2B). These data reveal that the peripheral application of TFP suppressed peripheral and central inflammation. Notably, acute LPS injection peripherally increased D2R mRNA expression in the hypothalamus at 6 h (Fig. 3A). Although the suppression of LPS-induced upregulation of D2R mRNA expression by TFP was not statistically significant, hypothalamic D2R mRNA expression in the LPS-TFP group tended to decrease (Fig. 3A).

Trifluoperazine decreases plasma TNF- α and restores blood glucose homeostasis in obese mice

Chronic HFD feeding over 2 months acts as the causal regulator to trigger prolonged microglial activation in the hypothalamic ARC ¹². An increase in D2R immunoreactivity in the hypothalamic area, especially the ARC, was detected at 12 weeks after HFD feeding when compared to that examined in the chow group (Fig. 3B, arrows). This finding, in conjunction with the results shown in Fig. 3A, demonstrates that peripheral inflammation either induced by LPS challenge or chronic HFD feeding can trigger D2R expression in the hypothalamus. Accordingly, daily administration of TFP in mice through the i.p. route started at 12 weeks post HFD feeding and continued for 4 weeks (Fig. 4A). The plasma levels of TNF- α and IL-1 β were measured at the end of the experiments. As shown in Fig. 4B, chronic HFD feeding increased plasma TNF- α and IL-1 β . Plasma TNF- α levels declined efficiently after TFP treatment for 4 weeks, although TFP decreased the amount of plasma IL-1 β to a lesser extent. We noticed that the body weight of obese mice was not changed by administration of TFP (Fig. 5A).

Next, we found that chronic HFD feeding for 16 weeks caused hyperglycemia, hyperinsulinemia, and high plasma levels of LDL/VLDL, TG, and HDL in obese mice (Fig. 5B-F). Moreover, the amount of WAT and BAT was significantly increased in obese mice fed a HFD for 16 weeks (Fig. 5G, H). However, daily administration of TFP for 4 weeks effectively diminished the plasma levels of glucose and insulin in obese mice (Fig. 5B and C). However, TFP application did not influence the WAT and BAT of obese mice or the plasma levels of LDL/VLDL, triglycerides, or HDL in obese mice. The findings point to the promising effect of TFP on the regulation of glucose homeostasis in obesity.

Trifluoperazine suppresses HFD-induced gliosis in the hypothalamus

Furthermore, we examined microglial activation and astrocyte hypertrophy in the hypothalamic ARC at 16 weeks post HFD feeding and TFP treatment (Fig. 4A). Similar to the results shown in our previous study ¹², activated microglia with a larger cell size were observed in obese mice fed a HFD for 16 weeks when compared to those in the chow group (Fig. 6A, arrowheads); moreover, the activated microglia in the ARC of HFD-fed mice increased in number. However, 4 weeks of treatment with TFP significantly reduced the number of ARC microglia and their cell bodies (Fig. 6A, arrows). Chronic HFD feeding for 16 weeks not only caused astrocytic hypertrophy but also increased the intensity of astrocytes in the ARC compared to those observed in the chow-fed group (Fig. 6B, arrows). HFD-induced astrocytic activation was decreased after treatment with daily treatment with TFP for 4 weeks. Note that TFP application for 4 weeks caused insignificant alterations in microglia and astrocytes in the ARC of chow-fed mice. Altogether, daily

treatment with TFP for 4 weeks is effective in suppressing HFD-induced peripheral inflammation and ARC gliosis in obese mice.

Discussion

The findings from others have indicated that the inhibition of hypothalamic inflammation improves the control of glucose homeostasis ^{1,13,21}, pointing to the crucial role of hypothalamic inflammation in obesity-associated pathogenesis. Here, we show the anti-inflammatory action of TFP on peripheral and hypothalamic inflammation in obese mice. Although TFP administration did not reduce the body weight of the obese mice, this drug was able to attenuate obesity-associated hyperglycemia and restore plasma insulin levels back to the basal level.

Hypothalamic inflammation induced by HFD feeding has been linked to the development of obesity ^{8,9}. Moreover, the selective ablation of microglia in the ARC using the colony-stimulating factor 1 receptor (CSF1R) inhibitor PLX5622 is able to lessen HFD-triggered body weight gain and food intake ²². However, although microgliosis in the ARC was reduced after the peripheral application of TFP (1 mg/kg) for 1 month, there was no alteration in the body weight of obese mice with or without treatment with TFP. In past studies showing decreased body weight gain by the inhibition of microglial activation ²², either CSF1R inhibitor-induced selective ablation of microglia or genetic reduction in microglial inflammatory capacity to restrict hypothalamic inflammation was performed at the beginning of HFD feeding. In addition, the approach used to inhibit microglial proliferation for the prevention of central and peripheral inflammation using intracerebroventricular implantation of an Alzet osmotic minipump containing the antimetabolic drug arabinofuranosyl cytidine was conducted before HFD feeding ²³. Thus, perhaps TFP treatment should start at an earlier time point rather than 3 months later, since the animals have been through a 3-month course of HFD feeding at the beginning of TFP application. However, diet-induced body weight gain remained when the 4-week paradigm of TFP administration was performed in the beginning at 2 months after HFD feeding (Fig. S1A). The results shed light on the function of a 4-week treatment with TFP in blood glucose homeostasis but not in lipid metabolism.

Given that the effect of chronic HFD feeding on the upregulation of body weight, WAT and BAT was not blocked by a 4-week treatment with TFP, we reason that TFP action for 4 weeks at later time intervals with the continuous stimulation of HFD feeding might not change the animal behavior under HFD consumption conditions. This is supported by the observations that daily administration of TFP in HFD-fed mice did not alter their food intake in comparison with the HFD-vehicle group (Fig. S1B). Additionally, neuronal injury in the ARC has been observed in rats receiving a HFD for 1 week ⁸. Moreover, decreased cell numbers of proopiomelanocortin-producing neurons, a group of ARC neurons that suppress food intake, have been shown in mice after HFD feeding for 8 months ⁸. Perhaps chronic stimulation of HFD feeding in our study might perturb neural circuits that mediate energy expenditure and the food reward system. Thus, anti-peripheral inflammation or anti-gliosis by TFP in obese mice receiving long-term HFD feeding is not satisfactory to promote lipid metabolism and mitigate body weight gain.

Dopamine (DA) is well known to mediate immune responses in the periphery through its receptors expressed in immune cells ²⁴. High levels of brain DA and altered amounts of other neurotransmitters have been detected in obese animals compared to those in the lean group along with an increase in inflammatory mediators and oxidative markers ²⁵. TFP has been reported to inhibit cytokine release from LPS-stimulated macrophages and dendritic cells and acts as a potential anti-sepsis drug ¹⁵. This is consistent with our observations showing the anti-inflammatory effect of TFP on LPS-stimulated hypothalamic mixed glia and HFD-triggered peripheral inflammation. Moreover, endogenous expression of D2R was found in activated microglia in the infarct site after cerebral ischemia, in conjunction with an *in vitro* study, pointing to DA function in activated microglia-associated neuroinflammation ²⁶. Although HFD feeding for 4 weeks did not affect hypothalamic D2R gene expression ²⁷, our observation in this study indicated that chronic feeding of a HFD for 3 months increased D2R expression in the hypothalamic ARC. This raises the possibility that the inhibitory effect of TFP on the activation of microglia and astrocytes in the ARC of obese mice might occur through D2R action in peripheral immune cells and/or hypothalamic glial cells. Thus, based on our study shown here, D2R indeed can be a therapeutic target for obesity-associated inflammatory pathogenesis in the periphery and in the CNS.

This study shows that a 4-week program of TFP treatment effectively blocked the HFD-induced rise in blood glucose and maintained plasma insulin levels close to the control level. Thus, the results provide significant evidence to show the potential treatment paradigm of TFP for obesity-associated hyperglycemia through the inhibition of peripheral inflammation and ARC gliosis (Fig. 7).

Materials And Methods

Cell culture

Primary microglia were collected from mixed glial cultures that were prepared via homogenization of cortical tissues dissected from rat pups at postnatal day (PD) 1-2 ²⁸. The tissues were filtered through a 70-mm nylon filter mesh, and after centrifugation, the cell pellet was re-suspended in DMEM/F-12 medium (Thermo Fisher Scientific) containing 10% fetal bovine serum (Gibco). The cells were seeded onto poly-D-lysine (Sigma-Aldrich)-coated T-75 culture flasks and incubated in 5% CO₂ at 37°C for 7-8 days. After microglia were collected using the shake-off method, these cells were re-plated onto coverslips in 24-well plates at a density of 5 x 10⁴ cells/well or in 60-mm Petri dishes at a density of 1 x 10⁶ cells/dish in DMEM/F-12 medium containing 10% FBS for 3 h. The cultures were treated with 1 mM TFP (Sigma-Aldrich) in the presence of LPS (10 ng/ml; Sigma-Aldrich) in DMEM containing N1 serum supplement (Thermo Fisher Scientific) for 3 h to examine isolectin B4 (IB4) and immunofluorescence for *inducible nitric oxide synthase* (iNOS) or for 6 h to investigate TNF-α and IL-1β mRNA expression. Alternatively, mouse mixed glia were prepared from the hypothalamus of pups at the age of PD 1-2 and re-plated onto PDL-coated coverslips in a 24-well plate at a density of 5 x 10⁴ cells per well. After incubation in 5% CO₂ at 37°C for 5 days, the cultures were treated in DMEM/F-12 medium without or with 1 mM TFP in the presence of LPS (10 ng/ml) for 3 h. The cultured media were collected for the

measurement of TNF- α and IL-1 β levels. Animal use for primary microglia preparation was approved by the National Cheng Kung University Institutional Animal Care and Use Committee, Tainan, Taiwan (IACUC approval number: 106060). The methods were performed in accordance with relevant guidelines and regulations.

Animals

Eight-week-old male C57BL/6 mice were purchased from National Cheng Kung University Laboratory Animal Center (<http://www.ncku.edu.tw/animal/eng/nckulac.html>), and randomly paired-housed in cages with free access to food and water *ad libitum* under standard room conditions (room temperature: $23\pm 2^{\circ}\text{C}$; humidity: $58\pm 2\%$; 12-h light/dark cycle). To induce obesity in mice, the animals were fed a HFD containing 61.6% kcal from fats, 18.1% from proteins and 20.3% from carbohydrates (Rodent Purified Diet #58Y1; TestDiet, St. Louis, MO, USA). The animals receiving a normal diet (Laboratory Rodent Diet #5001; LabDiet, St. Louis, MO, USA) were referred to as the chow group. All the experiments were performed in compliance with ARRIVE (Animal Research: Reporting In Vivo Experiments) Guidelines (<https://www.nc3rs.org.uk/arrive-guidelines>) and strictly following the 3Rs (Replacement, Reduction and Refinement) to avoid unnecessary sacrifice. Animal experiments through the performance of the following methods were approved by the National Cheng Kung University Institutional Animal Care and Use Committee, Tainan, Taiwan (IACUC approval number: 106060). The animals were anesthetized and sacrificed by i.p. injection with Zoletil 50 (Virbac Taiwan Co., Ltd.; 5X dilution in saline, 0.05-0.06 ml/10 g). The choice of anesthetics was recommended by the veterinary specialist at the university animal center to effectively reduce pain in animals. The experimental protocol is outlined in Fig. S2.

Peripheral injection of LPS and TFP

Injection of LPS (1 mg/kg) by the i.p. route combined with saline or TFP (2 mg/kg) was performed on 8-week-old C57BL/6 mice. Animals that received saline served as the control group (vehicle). Blood samples were collected at 3 h from the retro-orbital sinuses of anesthetized mice using a heparinized capillary tube²⁹. Alternatively, under anesthesia, blood samples were collected at 6 h via cardiac puncture using a 26G needle rinsed with 10 ml of heparin (5000 IU/mL; Leo Pharmaceutical, Ltd., Denmark). Animals were then sacrificed, and hypothalamic tissues were removed for measurement of TNF- α and IL- β mRNA levels.

TFP (2 mg/kg/injection) administration through the i.p. route began at 12 weeks post HFD feeding, and the daily injection continued for 4 weeks. The animal groups include chow-vehicle, HFD-vehicle, chow-TFP, and HFD-TFP. Blood samples and brains were collected after animals were anesthetized.

Measurement of cytokines

The mixed glial culture media or blood samples from mice were collected at the different experimental time points as described above. After centrifugation, the supernatant was used to measure TNF- α and IL-

1b using a murine TNF- α Quantikine ELISA Kit and murine IL-1b/IL-1F2 Quantikine ELISA Kit following the protocol provided by the vendor (R&D system; Table 1).

Assays for metabolic indices

The blood samples used for the measurement of glucose were collected using a heparinized capillary tube from animals after fasting for 15 h. Roche Accu-Chek® blood glucose meters were used to measure the amount of blood glucose in the animal groups. In addition, the blood samples collected from the fasting animals were centrifuged, and the supernatant was used to measure plasma insulin (Table 1) and other metabolic markers, including high-density lipoprotein (HDL), low-density lipoprotein/very-low-density lipoprotein (LDL/VLDL), and triglyceride (TG), using Quantification Colorimetric/Fluorometric Kits (Table 1).

Collection of adipose tissues

After perfusion, white adipose tissue (WAT) was collected from epididymal adipose tissue, and brown adipose tissue (BAT) was collected from interscapular brown adipose tissue for weight measurement on an electronic analytical balance (ATX224; SHIMADZU, Japan).

Quantitative real-time polymerase chain reaction (QPCR)

Animals were anesthetized with Zoletil 50 (Virbac Taiwan Co., Ltd.; 5X dilution in saline, 0.05-0.06 ml/10 gm) by i.p. injection and then perfused with 0.9% saline in diethylpyrocarbonate (DEPC; Sigma)-treated distilled water. Hypothalamic tissues were removed and homogenized in TRIzol™ (Invitrogen) for RNA extraction. cDNA generation using MMLV reverse transcriptase (Invitrogen) and PCR amplification by Fast SYBR® Green Master Mix (Applied Biosystems) were previously described³⁰. We used Primer-BLAST software provided by the National Center for Biotechnology Information to design primers that were manufactured by Taiwan Genomics. The level of cyclophilin A (CyPA) was used as an internal control. StepOne Software v2.1 (Applied Biosystems) was used to determine the cycle threshold fluorescence values. The expression level of the target genes relative to the internal control is presented as $2^{-\Delta CT}$, where $\Delta CT = (Ct \text{ target gene} - Ct \text{ CyPA})$. The sequences of the specific primers for TNF- α , IL-1b, D2R, and Cyclophilin A (CyPA) are as follows: rat TNF- α (NM_012675): Forward 5'-CATCCGTTCTCTACCCAGCC-3', Reverse 5'-AATTCTGAGCCCGGAGTTGG-3'; rat IL-1b (NM_031512.2): Forward 5'-CCTATGTCTTGCCCGTGGAG-3' Reverse 5'-CACACACTAGCAGGTCGTCA-3'; rat CyPA (NM_017101.1): Forward 5'-CGTCTGCTTCGAGCTGTTTG-3', Reverse 5'-GTAAAATGCCCCGCAAGTCAA-3'; murine TNF- α (NM_008361.4) Forward 5'-CCGGACTCCGCAAAGTCTAA-3', Reverse 5'-ACCGTCAGCCGATTTGCTAT-3'; murine IL-1b (NM_008361.4): Forward 5'-TGCCACCTTTTGACAGTGATGA-3', Reverse 5'-AAGGTCCACGGGAAAGACAC-3'; murine D2R (NM_010077.3): Forward 5'-CCATTGTCTGGGTCCTGTCC-3', Reverse 5'-CTGCTACGCTTGGTGTGAC-3'; and murine CyPA (NM_008907.1): Forward 5'-CGTCTGCTTCGAGCTGTTTG-3', Reverse 5'-GTAAAATGCCCCGCAAGTCAA-3'.

Double immunofluorescence

The cell cultures were fixed in PBS containing 4% paraformaldehyde for 10 min and then treated with 0.1% Triton-X-100 in PBS at room temperature for 30 min. Rat microglia were incubated with rabbit anti-iNOS antibody (1:400) and biotin-conjugated IB4 (1:200) in PBS containing 5% horse serum overnight at 4°C, followed by biotinylated anti-rabbit IgG (1:200) for anti-iNOS antibody and Alexa Fluor 488 (1:200) for IB4 for 1 h at room temperature. The cultures were incubated with PBS containing Cy3–avidin (1:200) for another 45 min. Alternatively, mouse mixed glial cells were incubated with anti-GFAP antibody (1:400) and biotin-conjugated IB4 (1:200) overnight at 4°C. The cells were reacted with biotinylated anti-rabbit IgG (1:200) and Alexa Fluor 488 (1:200) at room temperature for 1 h and then Cy3-avidin (1:200) for another 45 min. The immunostained cells were visualized and photographed under a Nikon E800 fluorescence microscope equipped with a CCD camera. The antibodies are listed in Table 1.

Brain tissue immunostaining

The brain samples removed from animals were fixed overnight in 4% paraformaldehyde and then transferred to tubes containing 30% (w/v) sucrose in PBS until the tissues sank to the bottom of the tube. The tissues were mounted in Tissue Tek optimal cutting temperature compound (Electron Microscopy Sciences, Torrance, CA, USA) and then sectioned at 20-μm thickness. The floating brain sections were treated with 1% Triton-X-100 in PBS at 4°C overnight, followed by incubation with primary antibodies in PBS containing 0.1% Triton X-100 and 1% horse serum at 4°C overnight. The tissue sections were then incubated with biotinylated secondary antibodies for 1 h and with Alexa Fluor 488 or Cy3–avidin (1:200) for another 45 min. The immunostained tissues were observed under an Olympus FLUOVIEW FV1000 confocal laser scanning microscope (FV1000, Japan) at wavelengths of 405, 488 or 594 nm. The primary antibodies used in the study are listed in Table 1. Alternatively, brain sections were *permeabilized* in 0.3% Triton-X-100 in PBS for 30 min, incubated with rabbit anti-D2R antibody (Table 1) in PBS at 4°C overnight, and treated with biotinylated anti-rabbit IgG (1:200) in PBS for 1 h. The brain sections were then reacted with Vectastain ABC reagent (Vector Labs; Cat# PK-6100) containing 3,3'-diaminobenzidine and nuclear counterstaining by hematoxylin. The immunostained sections were visualized and photographed under a Nikon E800 microscope equipped with a CCD camera.

Determination of microglial activation and astrocyte hypertrophy

The measurement of microglia and astrocyte activation was performed as previously described^{12,30}. The cell number and cell body size of Iba1⁺ microglia and the intensity of GFAP immunoreactivity in the ARC were analyzed using National Institutes of Health (NIH) ImageJ analysis software³¹. In general, randomly selected images per brain section were merged and captured in multiple 1-mm-thick steps using an Olympus FLUOVIEW FV1000 confocal laser scanning microscope. Images that were used for quantification were captured from 7-9 brain sections for Iba1 immunostaining and 6 brain sections for GFAP immunostaining from three animals per group. The microglial cell numbers are shown as the number of cells in an image with a size of 0.1 mm². The GFAP intensity data were normalized to those of the chow group (100%).

Statistical analysis

The presence of significant differences between each group (chow-vehicle, chow-TFP, HFD-vehicle, HFD-TFP) at different time points observed in this study was determined using one-way ANOVA with Sidak's multiple comparisons for the *in vivo* study or two-tailed Student's t test for *in vitro* experiments. Data are presented as the mean \pm SEM. The statistical significance was set as $P < 0.05$.

Abbreviations

ARC	arcuate nucleus
BAT	brown adipose tissue
CNS	central nervous system
CSF1R	colony-stimulating factor 1 receptor
CyPA	cyclophilin A
DA	dopamine
D2R	dopamine D2 receptor
ELISA	enzyme-linked immunosorbent assay
GFAP	glial fibrillary acidic protein
HDL	high-density lipoprotein
HFD	high-fat diet
LDL/VLDL	low-density lipoprotein/very-low-density lipoprotein
IB4	isolectin B4
IL-1b	interleukin-1b
IL-6	interleukin-6
iNOS	inducible nitric oxide synthase
i.p.	intraperitoneal
LPS	lipopolysaccharide
NIH	National Institutes of Health
QPCR	quantitative real-time polymerase chain reaction
TFP	trifluoperazine
TG	triglyceride
TNF-a	tumor necrosis factor-a
WAT	white adipose tissue

Declarations

Acknowledgments

The authors thank Ms. Chia-Hsin Ho for technical assistance and the “Bio-image Core Facility of the National Core Facility Program for Biotechnology, Ministry of Science and Technology, Taiwan,” for technical services provided.

Funding

This work was supported by the Ministry of Science and Technology, Taiwan (MOST 108-2320-B-006-003 and 109-2811-B-006-533).

Author Contributions

HTH designed the experiment, conducted the data analysis and wrote the manuscript. SFT, the senior author, provided oversight, experimental design, result interpretation, and manuscript preparation/editing. PCC, PSC, and YMK participated in the discussion, experimental design, and materials. WTC assisted with imaging analysis. All authors read and approved the final manuscript.

Ethics Declaration

Conflicts of Interest

The authors declare that they have no competing interests.

Ethics Approval

The animal study was approved by the National Cheng Kung University Institutional Animal Care and Use Committee, Tainan, Taiwan (IACUC approval number: 106060).

References

1. Miller, A. A. & Spencer, S. J. Obesity and neuroinflammation: a pathway to cognitive impairment. *Brain Behav Immun.* **42**, 10–21 <https://doi.org/10.1016/j.bbi.2014.04.001> (2014).
2. Konner, A. C., Klockener, T. & Bruning, J. C. Control of energy homeostasis by insulin and leptin: targeting the arcuate nucleus and beyond. *Physiol Behav.* **97**, 632–638 <https://doi.org/10.1016/j.physbeh.2009.03.027> (2009).
3. Sohn, J. W., Elmquist, J. K. & Williams, K. W. Neuronal circuits that regulate feeding behavior and metabolism. *Trends Neurosci.* **36**, 504–512 <https://doi.org/10.1016/j.tins.2013.05.003> (2013).
4. Hotamisligil, G. S. Inflammation and metabolic disorders. *Nature.* **444**, 860–867 <https://doi.org/10.1038/nature05485> (2006).

5. Kanneganti, T. D. & Dixit, V. D. Immunological complications of obesity. *Nature immunology*. **13**, 707–712 <https://doi.org/10.1038/ni.2343> (2012).
6. Pimentel, G. D., Ganeshan, K. & Carnevali, J. B. Hypothalamic inflammation and the central nervous system control of energy homeostasis. *Molecular and cellular endocrinology*. **397**, 15–22 <https://doi.org/10.1016/j.mce.2014.06.005> (2014).
7. Purkayastha, S. & Cai, D. Neuroinflammatory basis of metabolic syndrome. *Molecular metabolism*. **2**, 356–363 <https://doi.org/10.1016/j.molmet.2013.09.005> (2013).
8. Thaler, J. P. *et al.* Obesity is associated with hypothalamic injury in rodents and humans. *J Clin Invest*. **122**, 153–162 <https://doi.org/10.1172/JCI59660> (2012).
9. Baufeld, C., Osterloh, A., Prokop, S., Miller, K. R. & Heppner, F. L. High-fat diet-induced brain region-specific phenotypic spectrum of CNS resident microglia. *Acta neuropathologica*. **132**, 361–375 <https://doi.org/10.1007/s00401-016-1595-4> (2016).
10. Chowen, J. A., Argente, J. & Horvath, T. L. Uncovering novel roles of nonneuronal cells in body weight homeostasis and obesity. *Endocrinology*. **154**, 3001–3007 <https://doi.org/10.1210/en.2013-1303> (2013).
11. Jastroch, M., Morin, S., Tschop, M. H. & Yi, C. X. The hypothalamic neural-glial network and the metabolic syndrome. *Best Pract Res Clin Endocrinol Metab*. **28**, 661–671 <https://doi.org/10.1016/j.beem.2014.02.002> (2014).
12. Huang, H. T. *et al.* Chronic exposure to high fat diet triggers myelin disruption and interleukin-33 upregulation in hypothalamus. *BMC Neurosci*. **20**, 33 <https://doi.org/10.1186/s12868-019-0516-6> (2019).
13. Milanski, M. *et al.* Saturated fatty acids produce an inflammatory response predominantly through the activation of TLR4 signaling in hypothalamus: implications for the pathogenesis of obesity. *The Journal of neuroscience: the official journal of the Society for Neuroscience*. **29**, 359–370 <https://doi.org/10.1523/JNEUROSCI.2760-08.2009> (2009).
14. Marques, L. O., Lima, M. S. & Soares, B. G. Trifluoperazine for schizophrenia. *Cochrane Database Syst Rev*. **CD003545**, <https://doi.org/10.1002/14651858.CD003545.pub2> (2004).
15. Park, J. H. *et al.* Repositioning of the antipsychotic drug TFP for sepsis treatment. *J Mol Med (Berl)*. **97**, 647–658 <https://doi.org/10.1007/s00109-019-01762-4> (2019).
16. Roudebush, R. E., Berry, P. L., Layman, N. K., Butler, L. D. & Bryant, H. U. Dissociation of immunosuppression by chlorpromazine and trifluoperazine from pharmacologic activities as dopamine antagonists. *Int J Immunopharmacol*. **13**, 961–968 [https://doi.org/10.1016/0192-0561\(91\)90049-d](https://doi.org/10.1016/0192-0561(91)90049-d) (1991).
17. Xia, Y. *et al.* Antipsychotic Drug Trifluoperazine Suppresses Colorectal Cancer by Inducing G0/G1 Arrest and Apoptosis. *Front Pharmacol*. **10**, 1029 <https://doi.org/10.3389/fphar.2019.01029> (2019).
18. Yang, T. T. *et al.* Differential distribution and activation of microglia in the brain of male C57BL/6J mice. *Brain Struct Funct*. **218**, 1051–1060 <https://doi.org/10.1007/s00429-012-0446-x> (2013).

19. Borovikova, L. V. *et al.* Vagus nerve stimulation attenuates the systemic inflammatory response to endotoxin. *Nature*. **405**, 458–462 <https://doi.org/10.1038/35013070> (2000).
20. Qin, L. *et al.* Systemic LPS causes chronic neuroinflammation and progressive neurodegeneration. *Glia*. **55**, 453–462 <https://doi.org/10.1002/glia.20467> (2007).
21. Posey, K. A. *et al.* Hypothalamic proinflammatory lipid accumulation, inflammation, and insulin resistance in rats fed a high-fat diet. *American journal of physiology. Endocrinology and metabolism*. **296**, E1003–1012 <https://doi.org/10.1152/ajpendo.90377.2008> (2009).
22. Valdearcos, M. *et al.* Microglial Inflammatory Signaling Orchestrates the Hypothalamic Immune Response to Dietary Excess and Mediates Obesity Susceptibility. *Cell metabolism* **26**, 185–197 e183, [doi:10.1016/j.cmet.2017.05.015](https://doi.org/10.1016/j.cmet.2017.05.015) (2017).
23. Andre, C. *et al.* Inhibiting Microglia Expansion Prevents Diet-Induced Hypothalamic and Peripheral Inflammation. *Diabetes*. **66**, 908–919 <https://doi.org/10.2337/db16-0586> (2017).
24. Arreola, R. *et al.* Immunomodulatory Effects Mediated by Dopamine. *Journal of immunology research* 2016, 3160486, [doi:10.1155/2016/3160486](https://doi.org/10.1155/2016/3160486) (2016).
25. Labban, R. S. M. *et al.* High-fat diet-induced obesity and impairment of brain neurotransmitter pool. *Translational neuroscience*. **11**, 147–160 <https://doi.org/10.1515/tnsci-2020-0099> (2020).
26. Huck, J. H. *et al.* De novo expression of dopamine D2 receptors on microglia after stroke. *Journal of cerebral blood flow and metabolism: official journal of the International Society of Cerebral Blood Flow and Metabolism*. **35**, 1804–1811 <https://doi.org/10.1038/jcbfm.2015.128> (2015).
27. de Leeuw, J. E. *et al.* Four weeks high fat feeding induces insulin resistance without affecting dopamine release or gene expression patterns in the hypothalamus of C57Bl6 mice. *Brain research*. **1250**, 141–148 (2009).
28. Wang, C. Y., Hsieh, Y. T., Fang, K. M., Yang, C. S. & Tzeng, S. F. Reduction of CD200 expression in glioma cells enhances microglia activation and tumor growth. *J Neurosci Res*. **94**, 1460–1471 <https://doi.org/10.1002/jnr.23922> (2016).
29. Tsai, S. F. *et al.* Stress Aggravates High-Fat-Diet-Induced Insulin Resistance via a Mechanism That Involves the Amygdala and Is Associated with Changes in Neuroplasticity. *Neuroendocrinology*. **107**, 147–157 <https://doi.org/10.1159/000491018> (2018).
30. Huang, H. T., Chen, P. S., Kuo, Y. M. & Tzeng, S. F. Intermittent peripheral exposure to lipopolysaccharide induces exploratory behavior in mice and regulates brain glial activity in obese mice. *J Neuroinflammation*. **17**, 163 <https://doi.org/10.1186/s12974-020-01837-x> (2020).
31. Rueden, C. T. *et al.* ImageJ2: ImageJ for the next generation of scientific image data. *BMC bioinformatics*. **18**, <https://doi.org/10.1186/s12859-017-1934-z> (2017).

Tables

Table 1. List of reagents (antibodies and assay kits) in the study

Reagents	Manufacturer (RRID)
Polyclonal rabbit anti-D2R	Biorbyt, Cat# orb10515, RRID:AB_10747533
Polyclonal rabbit anti-GFAP antibody	Millipore, RRID:AB_2109645
Polyclonal rabbit anti-Iba1 antibody	Wako, RRID:AB_839504
Polyclonal rabbit anti-iNOS antibody	Calbiochem, RRID: AB_212220
Biotin-conjugated isolectin B4 (IB4)	Sigma-Aldrich, Cat#L2140
Biotinylated anti-rabbit IgG	Abcam, RRID: AB_954902
Cy3-conjugated Streptavidin	Thermo Fischer, Cat#434315
Alexa Fluo 488- Streptavidin	Thermo Fisher, RRID: AB_2336881
Mouse TNF- α Quantikine ELISA Kit	R&D Systems, RRID:AB_2877064
Mouse IL-1 β /IL-1F2 Quantikine ELISA Kit	R&D Systems, Cat# MLB00C
Mercodia Mouse Insulin ELISA Kit	Mercodia, RRID: AB_2783837
HDL and LDL/VLDL Quantification Colorimetric/Fluorometric Kit	BioVision, Cat# K613
Triglyceride Quantification Colorimetric/Fluorometric Kit	BioVision, Cat# K622

IF: immunofluorescence

Figures

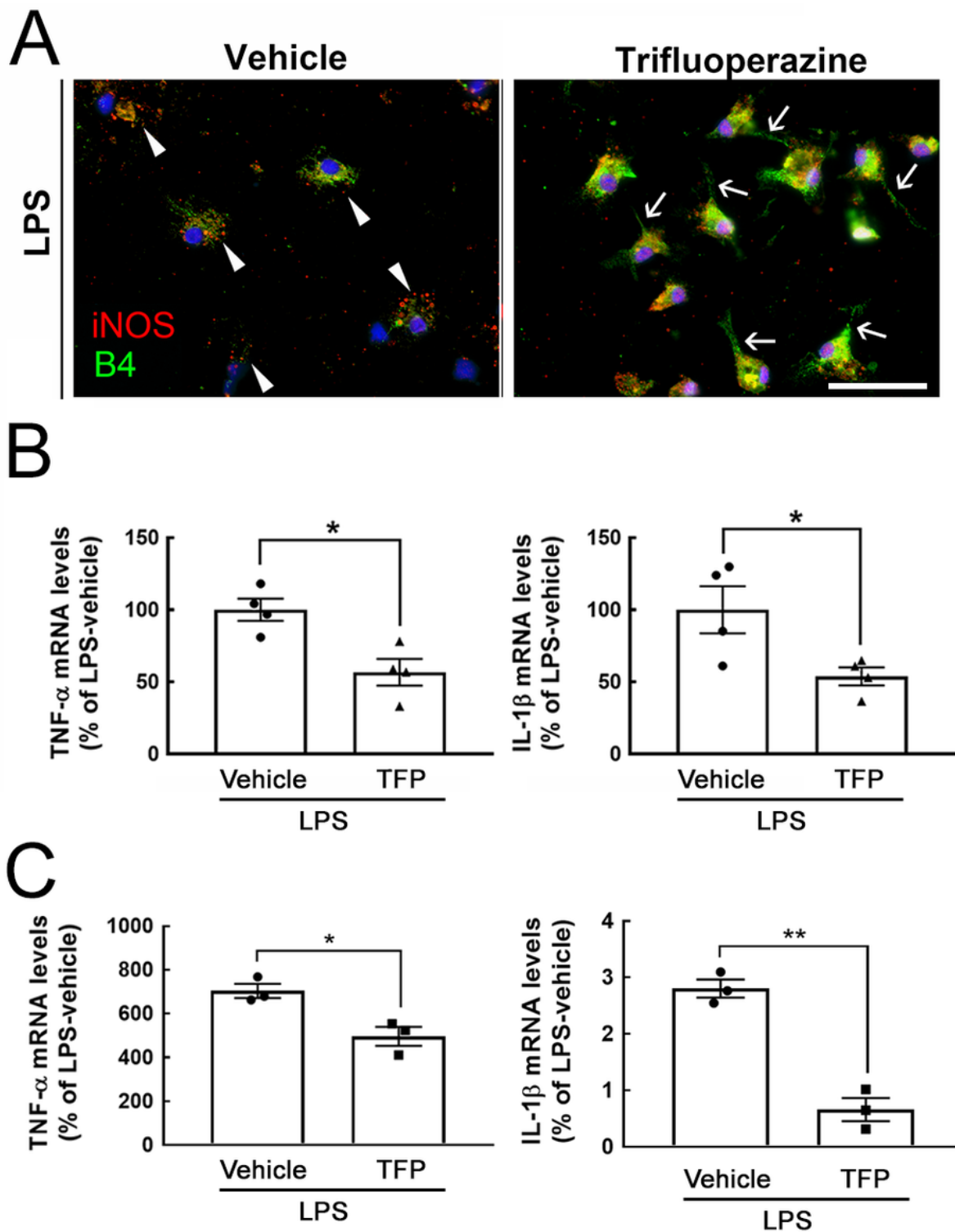


Figure 1

Exposure to TFP suppresses the expression of proinflammatory mediators in glia cultures. (A) Rat microglia were treated 10 ng/ml of LPS and 1 μ M of TFP for 3 h, and then subjected to immunostaining for iNOS (red) and IB4 staining (green) as described in Materials and Methods. Arrowheads indicate iNOS expression significantly in amoeboid microglia, and arrows show microglia with extending cell processes. Scale bar in A = 50 μ m. (B) Rat microglia were treated with vehicle or TFP in the presence of LPS for 6 h,

and then their TNF- α and IL-1 β mRNA expression was measured by QPCR as described in Materials and Methods. (C) Hypothalamic mixed glia cells were treated with 1 μ M TFP in the presence of LPS (10 ng/ml) for 3 h. The levels of TNF- α and IL-1 β in the culture medium were measured using ELISA kits. The data are presented in (B; n=4 experiments) and (C; n=3 experiments) as the mean \pm SEM. *p<0.05 versus vehicle.

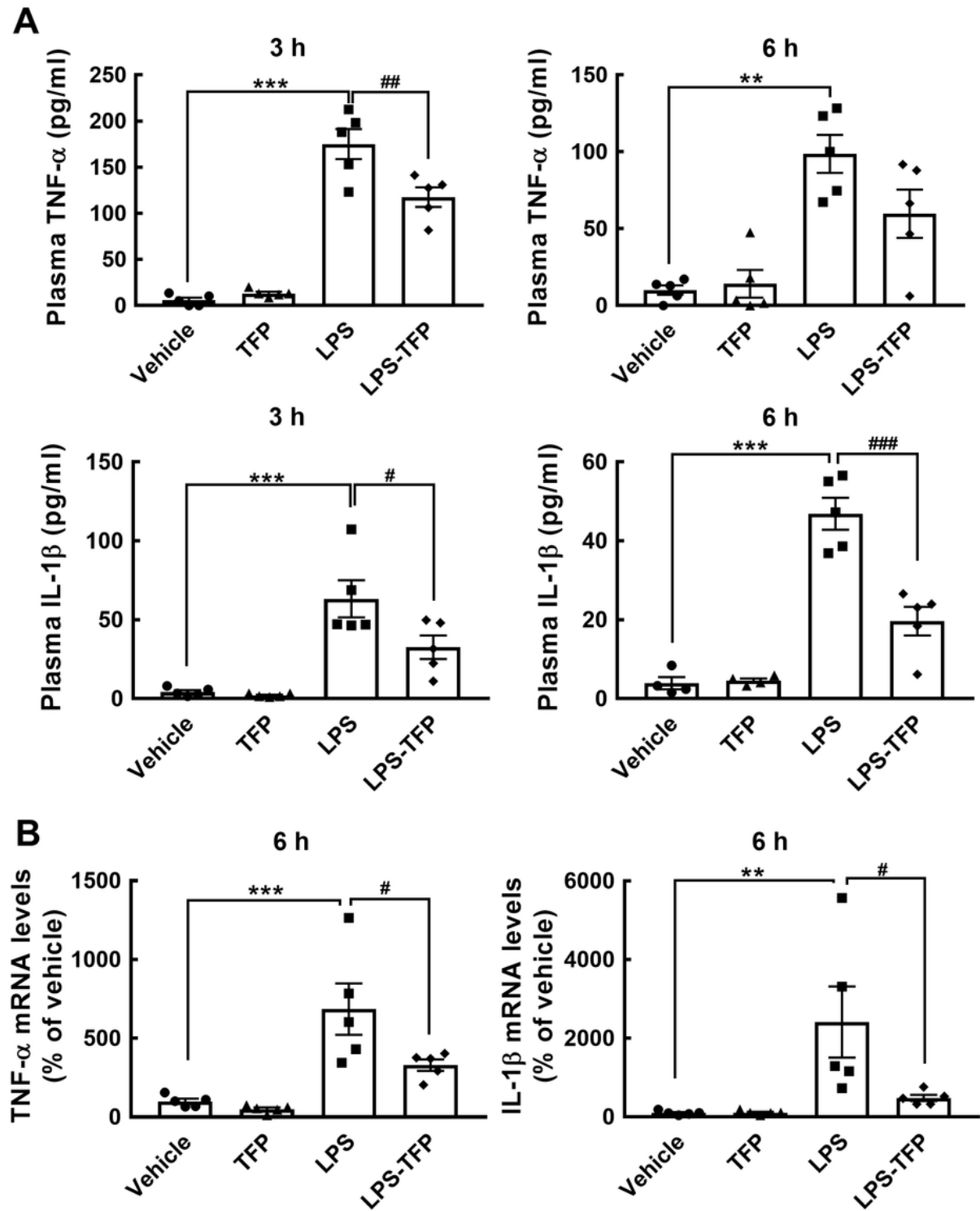
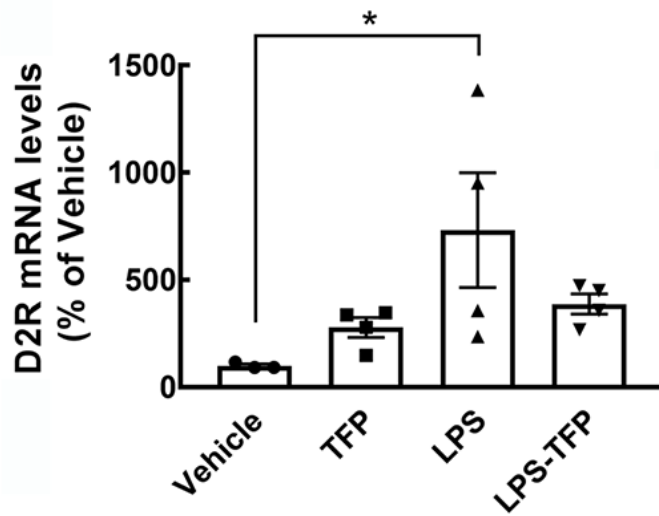


Figure 2

TFP inhibits LPS-induced production of TNF- α and IL-1 β in the plasma and hypothalamus. Animals were divided into four groups that received a bolus peripheral injection of vehicle, TFP (2 mg/kg), LPS (1 mg/kg), or LPS plus TFP. Blood samples from the four animal groups were collected at 3 and 6 h post injection for TNF- α and IL-1 β ELISAs (A), and then hypothalamic RNA isolation was conducted for the determination of TNF- α and IL-1 β mRNA expression (B) after animals were sacrificed at 6 h post injection. The data are presented as the mean \pm SEM (n=5 animals in each group). Samples from five animals per group were used for most assays, whereas samples from four animals were used for the IL-1 β ELISA at 6 h (A). Data are presented as the mean \pm SEM (n=5 animals for each group). Each dot represents one animal. *p<0.05, **p<0.01, ***p< 0.001 versus vehicle; #p<0.05, ##p<0.01 versus LPS.

A



B

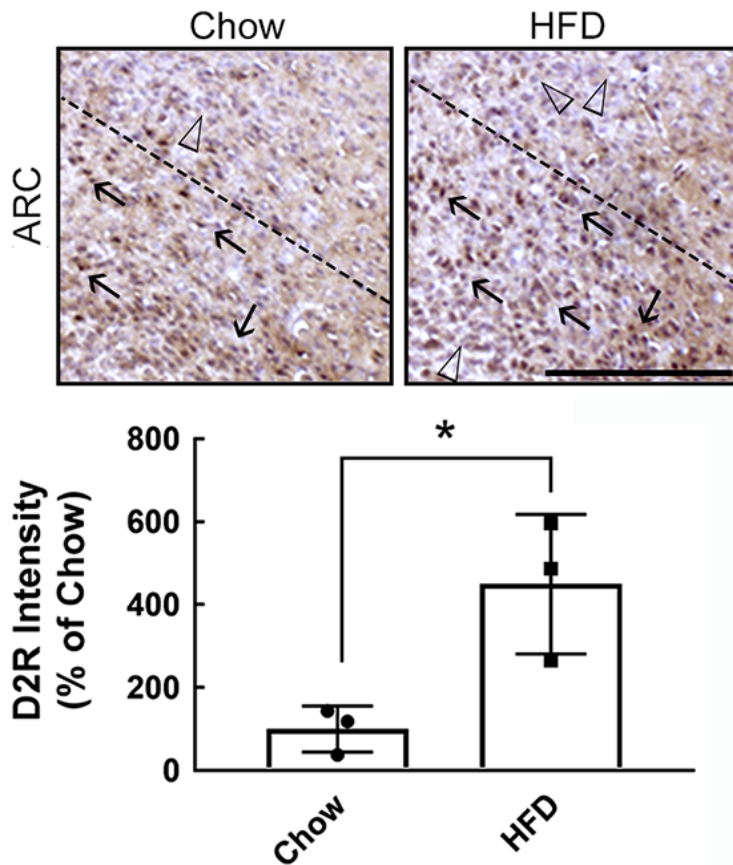


Figure 3

Increased expression of D2R in the hypothalamus after acute peripheral LPS injection or chronic HFD feeding. (A) Mice were injected peripherally with vehicle, TFP (2 mg/kg), LPS (1 mg/kg), or LPS plus TFP as described in the Materials and Methods. The hypothalamic tissues were removed at 6 h post injection for RNA extraction and QPCR analysis to determine the D2R mRNA expression. Each dot represents one animal. (B). Mice were sacrificed at 12 weeks after feeding with chow or HFD. Brain sections were

prepared as described in the Materials and Methods and subjected to immunohistochemistry for D2R expression. The arrows indicate D2R+ cells (brown) in the ARC, which mostly accumulate in HFD-fed mice. The observations were confirmed by quantification of D2R immunoreactive intensity in the ARC. The representative D2R– cells (blue) are shown by arrowheads above the dashed line. The results are presented in A and B as the mean \pm SEM (n = 3-4 animals for each group). Each dot represents one animal. *p<0.05 versus vehicle. Scale bar in B, 100 μ m.

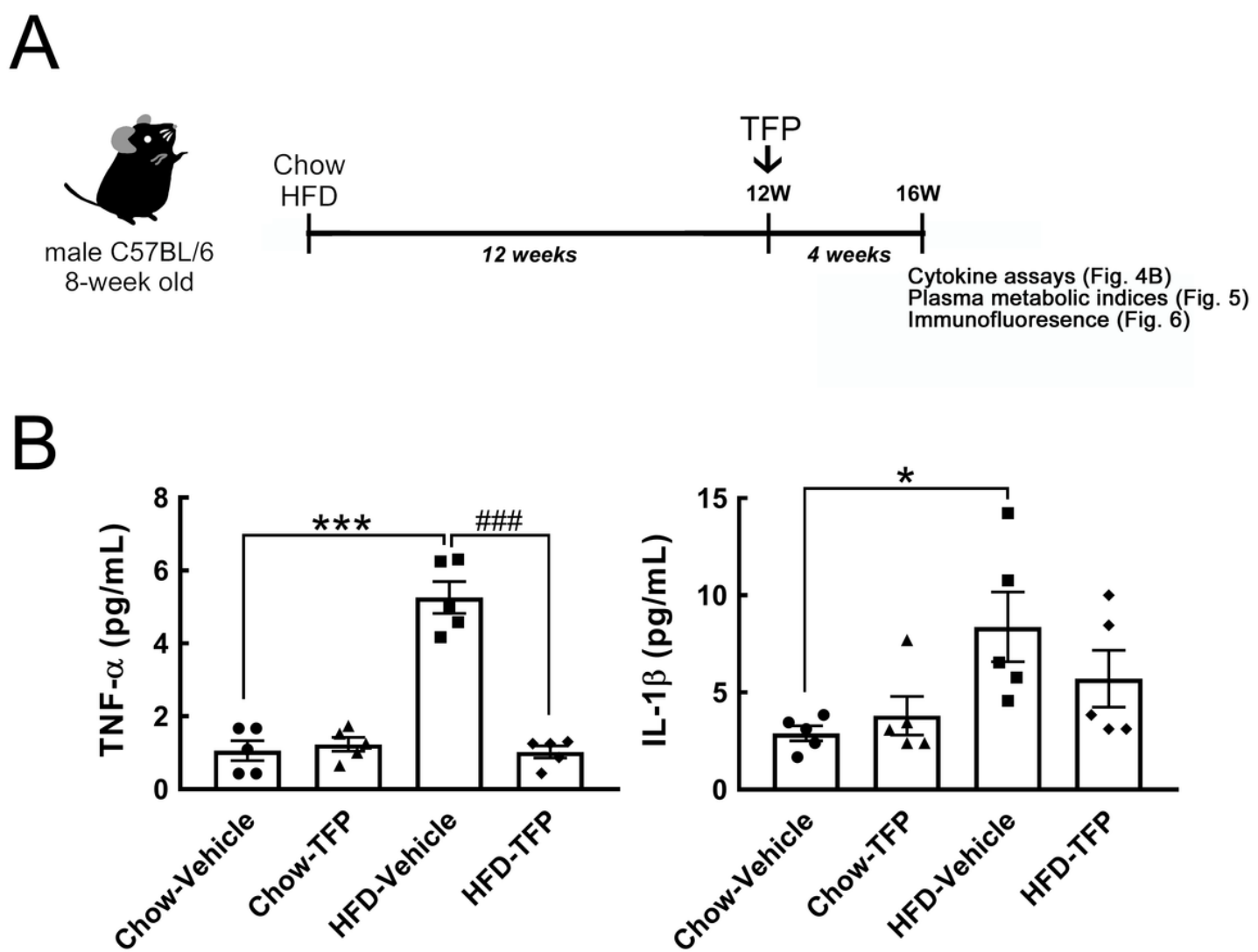


Figure 4

Decreased levels of plasma TNF- α and IL-1 β in obese mice treated with TFP for 4 weeks. (A) The schematic illustration shows that 8-week-old male C57BL/6 mice were fed chow or HFD for 12 weeks and then injected daily with TFP (2 mg/kg) via the i.p. route for another 4 weeks under chow or HFD feeding (chow-vehicle, chow-TFP, HFD-vehicle, HFD-TFP). At 16 weeks post feeding, blood samples were collected from animals without fasting for cytokine assays (B) and with fasting for the analysis of metabolic indices (Fig. 5). The brains were removed for sectioning and immunostaining (Fig. 6). (B) As indicated

above, the plasma samples were subjected to TNF- α or IL-1 β ELISA. Data are presented as the mean \pm SEM (n=5 animals for each group). Each dot represents one animal. *p<0.05, ***p< 0.001 versus chow-vehicle; ###p<0.001 versus HFD-vehicle.

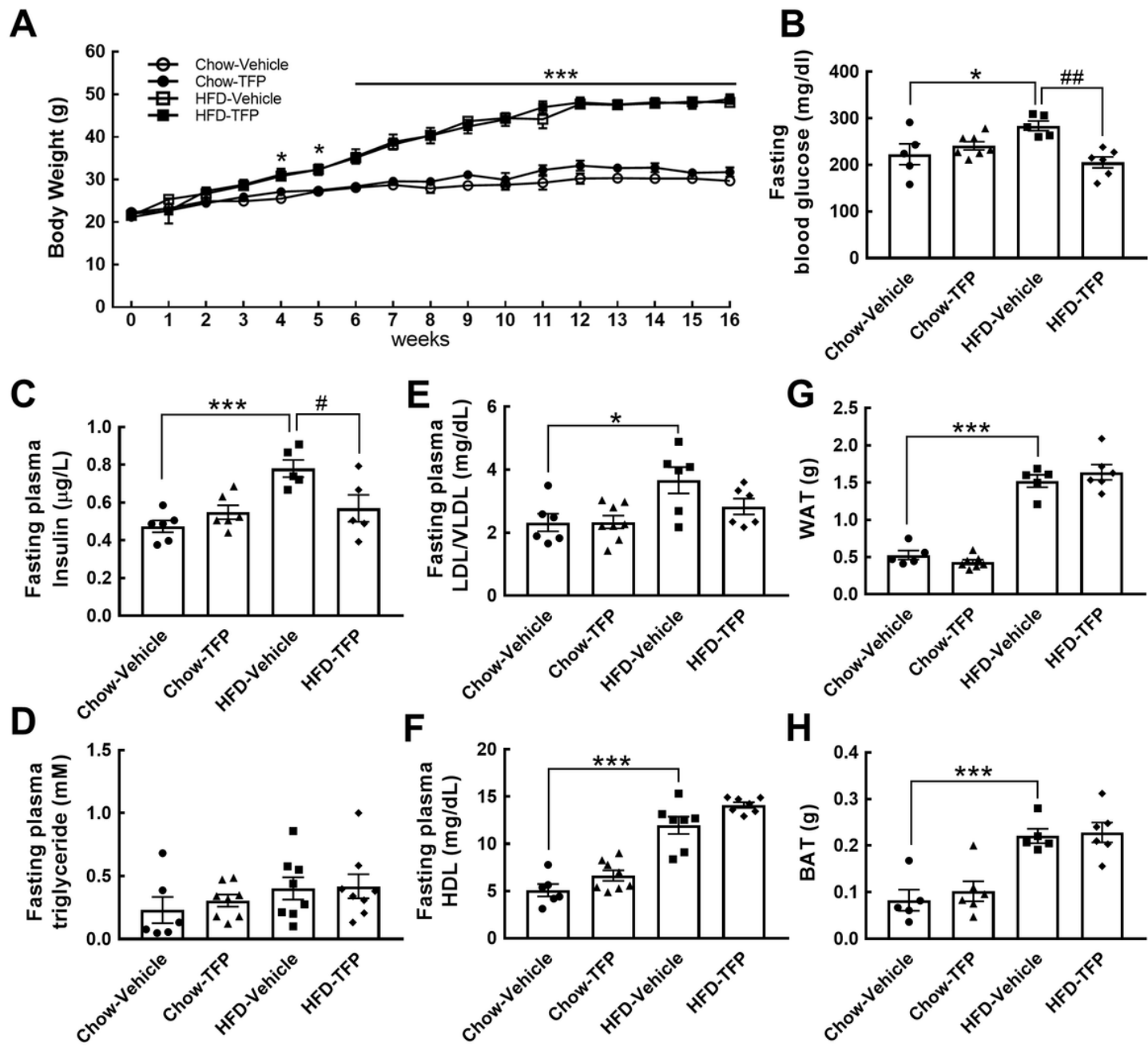


Figure 5

A rise in blood glucose and insulin by chronic HFD feeding was significantly suppressed by treatment with TFP for 4 weeks. (A) The body weights of the four animal groups were measured weekly. The body weight gain was significantly greater in HFD-fed animals treated with vehicle or TFP than in chow-fed animals treated with vehicle or TFP. Data are presented as the mean \pm SEM (n=6, chow-vehicle; n=8, chow-TFP, HFD-vehicle, or HFD-TFP). *p<0.05, ***p< 0.001 versus chow-vehicle. (B-H) At 16 weeks post feeding, the animals were fasted for 15 h, and then blood samples were collected as described in the

Materials and Methods. The samples were subjected to a series of assays including blood glucose (B), insulin (C), TG (D), LDL/VLDL (E), and HDL (F). In addition, WAT (G) and BAT (H) from the indicated sites in the Materials and Methods were weighed. The results are presented in B-H as the mean \pm SEM (n=5-8 animals for each group). Each dot represents one animal. *p<0.05, ***p< 0.001 versus chow-vehicle; #p<0.05, ##p<0.01 versus HFD-vehicle.

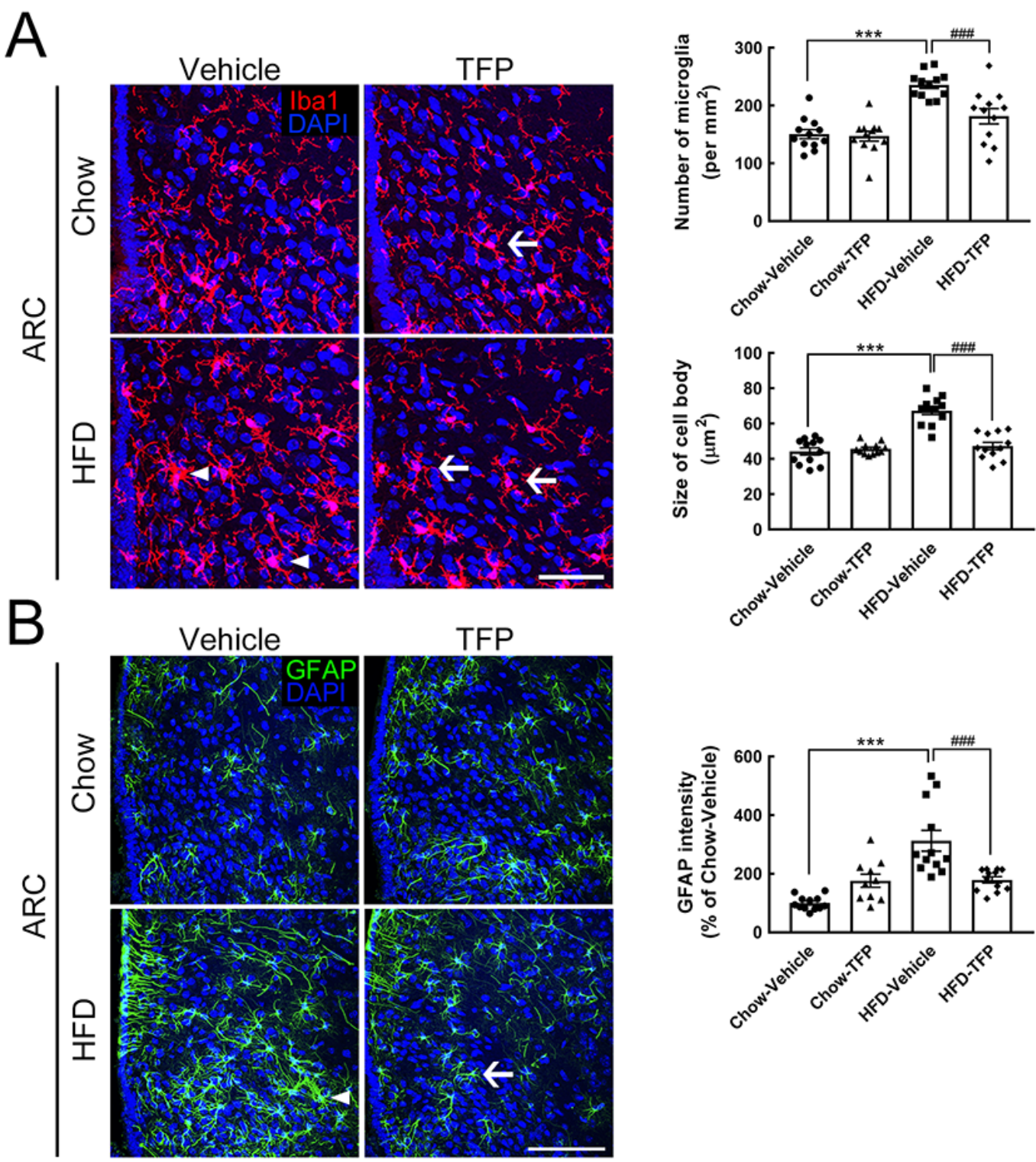


Figure 6

Microglial activation and astrocyte hypertrophy in the ARC of obese mice were attenuated by TFP treatment for 4 weeks. Brain tissue sections were prepared from the four animal groups at 16 weeks post feeding (Fig. 4A) and then subjected to Iba1 immunofluorescence (red in A) and GFAP immunofluorescence (green in B). DAPI nuclear counterstaining (blue in A and B) was conducted. Representative active microglia (A) and hypertrophic astrocytes (B) are indicated by arrowheads in the HFD-vehicle group. Arrows show microglia or astrocytes with a small size and fine processes in chow-TFP or HFD-TFP. The number of Iba1+ microglia in the ARC (per mm²) and their averaged cell size (μm²) in the four animal groups were measured. In addition, the average cell body size of microglia in the two regions was measured. In addition, the intensity of GFAP immunoreactivity in the ARC was quantified. The results are presented as the mean ± SEM (n=12 tissue sections for Iba1 immunostaining from 3 animals per group; n=9 tissue sections for GFAP immunostaining from 3 animals per group). Each dot represents one image. ***p< 0.001 versus chow-vehicle; #p<0.05, ##p<0.01, ###p<0.001 versus HFD-vehicle.

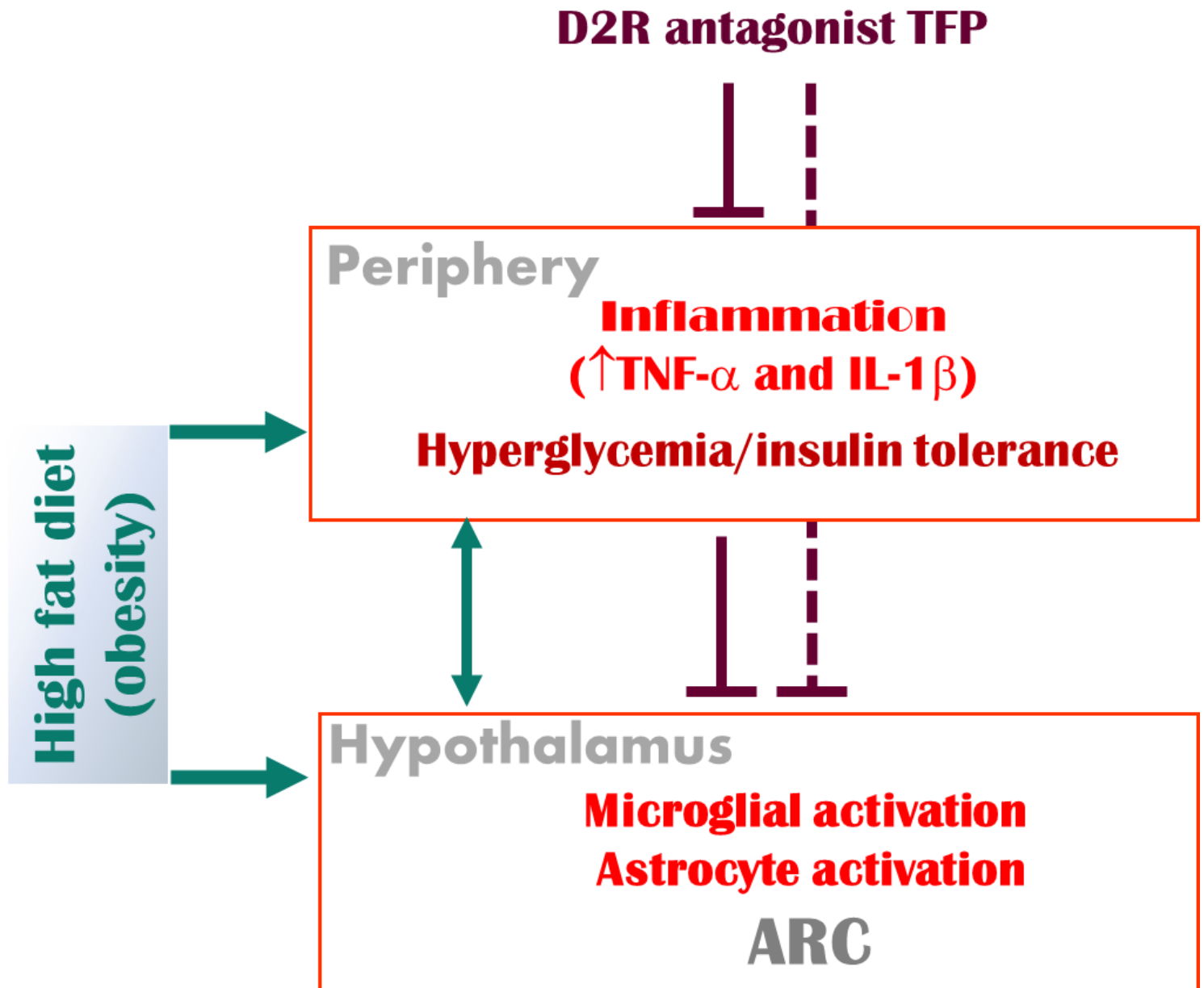


Figure 7

Schematic presentation shows the action of the antagonist TFP on the inhibition of obesity-associated peripheral inflammation, and on the suppression of the obesity-induced increase in blood glucose and insulin. Moreover, treatment with TFP enables the inhibition of HFD-induced gliosis in the ARC, an important hypothalamic region that regulates energy balance. The decrease in ARC gliosis might be because either peripheral inflammation was downgraded by TFP or by the direct effect of TFP on ARC glial cells.

Supplementary Files

This is a list of supplementary files associated with this preprint. Click to download.

- [SupplimentaryMaterials.doc](#)